New Developments in Multibody System Dynamics and Its Applications 2018 - Research Article

Advances in Mechanical Engineering

Advances in Mechanical Engineering
2019, Vol. 11(6) 1–12

DOI: 10.1177/1687814019857339
journals.sagepub.com/home/ade
SAGE

Variable formation control of multiple robots via VRc and formation switching to accommodate large heading changes by leader robot

Sung-Gil Wee[1], Yanyan Dai[2], Tae Hun Kang[1] and Suk-Gyu Lee[2]

Abstract

This article describes a novel multi-robot formation control based on a switching technique that allows follower robots to maintain formation when the leader robot's direction changes rapidly or unexpectedly. The formation pattern is determined using Virtual Robot's Center of the multi-robot formation. To avoid collision, the formation of robots reformed in optimal size by estimating the distance between the robot and an obstacle in real time. When the leader robot suddenly changes its direction, waypoints of follower robots are switched and the formation is quickly reconstructed. This prevents follower robots from colliding with each other and reduces their radius of movement and allows them to follow the leader robot at higher speed. The proposed method which is inherently a flexible control of multi-robot formation guarantees collision avoidance and prevents sudden changes in waypoints of the system by gradually changing its size. The validity of the proposed method is demonstrated via simulation and experimental results.

Keywords

Virtual Robot's Center, collision avoidance, formation switching, multi-robot formation

Date received: 28 January 2019; accepted: 22 May 2019

Handling Editor: Xiaoting Rui

Introduction

Multi-robot navigation in formation has received extensive attention in the past and been employed for various tasks, such as surveillance, inspection, factory automation, and logistics. Robots may be required to navigate in formation, for example, to maintain a communication network, to collaboratively manipulate deformable objects, or transportation of cable-suspended loads.[1–3] Flexible multi-robot formation control approaches can be classified depending on the knowledge of the initial positions of the robots. If the positions of robots are known, the positions and heading angles of the follower robots are estimated from the leader robot. In this case, the follower robots are controlled to maintain a constant distance from the leader robot and moves to the next position determined by the leader robot. In case that the initial positions of the robots are unknown, the robots move to form a targeted formation using fixed distances from arbitrary points, by sharing coordinating information on relative position and heading angles.[4]

Robots' obstacle avoidance which is a fundamental requirement for multi-robot formation has different approaches according to detection methods.[5–8] Jin

[1]DGIST, Daegu, Republic of Korea
[2]Department of Electrical Engineering, Yeungnam University, Gyeongsan, Republic of Korea

Corresponding author:
Yanyan Dai, Department of Electrical Engineering, Yeungnam University, 280 Daehak-Ro, Gyeongsan 712-749, Gyeongsangbuk, Republic of Korea.
Email: daiyanyan1011@gmail.com

et al.[9,10] proposed a new algorithm where robots navigate through surroundings of obstacle by recognizing detected obstacles as circles. Over the past decades, the control problems for mobile robots have been extensively studied. When designing controllers, depending on whether the non-linear dynamics are approximated/linearized, the control methods are classified into linear control and non-linear control. In Dai et al.,[11,12] robots avoid collision with obstacles as well as other robots based on predicted topography according to detected distances. In general multi-robot formations, robots share information on the positions of other robots for navigation. The robots use potential field method to avoid collision with other robots on overlapping paths or avoid path conflict by priority within detection range. In Dai et al.,[11] since non-linear control methods are developed on the basis of the original non-linear dynamical equations, they can maintain satisfactory control performance even when the state variables are far from the equilibrium point. According to Dai et al.,[12] because it is difficult for the dynamics of the robot to produce the perfect velocity as the kinematic controller, the dynamic controller is also used in this article. In Das and Kar,[13] a control structure that makes possible the integration of a kinematic controller and an adaptive fuzzy controller for trajectory tracking is developed for non-holonomic mobile robots. The system uncertainty, which includes mobile robot parameter variation and unknown non-linearities, is estimated by a fuzzy logic system. In practical point of view, this approach can be used for multi-robot formation effectively.

In this article, we propose a new formation maintenance method of mobile robots and the movement method for detection and avoidance of fixed obstacles. Under the proposed method where Virtual Robot's Center (VRc) determines the size of the formation of robots, robots can effectively change and restore the formation according to the geometry of the obstacle. The proposed formation is mainly determined by using the VRc of the multi-robot formation. Based on the position of the leader robot, follower robots form the equilateral triangle formation centered on the VRc. This makes it possible to change the formation of robots adaptively depending on the situation. In addition, when the leader robot suddenly changes its direction, follower robots switch their positions and effectively rapidly form a multi-robot formation in real time. As a result, since the moving radius of the follower robots is reduced drastically, follower robots maintaining a regular triangular pattern track leader robot fast.

Robot model

As in a mobile robot kinematics model,[14] the velocity and angular velocity of robot i, $(\dot{R}i)$, can be described

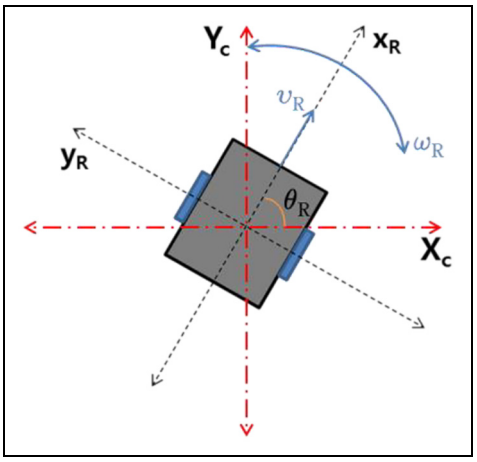

Figure 1. Coordinate system for a mobile robot in reference coordinate system.

using the linear velocity (v_R) and angular velocity (ω_R) of a differential mobile robot, as shown in equation (1). r is the radius of the wheel, L is the distance between the two wheels, and ω_l and ω_r are the rotational speeds of the respective wheels. Here, $v_{y_R}(i)$ is zero in a non-holonomic robot that cannot move to the y axis of v_R (Figure 1)

$$\dot{R}_i = \begin{bmatrix} v_{x_{R,i}} \\ v_{y_{R,i}} \\ \omega_{R,i} \end{bmatrix} = \mathrm{S}(R_i)v_i(\mathrm{t}) = \begin{bmatrix} r/2 & r/2 \\ 0 & 0 \\ r/L & -r/L \end{bmatrix} \begin{bmatrix} \omega_{l,i} \\ \omega_{r,i} \end{bmatrix} \tag{1}$$

Localization of a differential mobile robot is achieved via dead reckoning based on an odometer. Thus, it can be expressed by equations (2) and (3) according to the real robot's state and the predicted robot's state, respectively

$$\begin{aligned} R_i &= [x_{R,i} \quad y_{R,i} \quad \theta_{R,i}]^T \\ u_{i-1} &= [v_l \quad v_r]^T \\ \delta u_{i-1} &= [\delta_{v_l} \quad \delta_{v_r}]^T \end{aligned} \tag{2}$$

In equation (2), R is the position and direction of the ith real robot and u_{i-1} is the linear velocity of each wheel of the $i-1$th robot; it is also the odometry value. δu_{i-1} represents the linear velocity disturbance value of each wheel at the $i-1$th robot

$$\begin{aligned} \hat{R}_i &= \left[\hat{x}_{R,i} \quad \hat{y}_{R,i} \quad \hat{\theta}_{R,i}\right]^T \\ u_{i-1} &= [v_l \quad v_r]^T \\ \delta u_{i-1} &\sim N(m, \sigma^2) \end{aligned} \tag{3}$$

Equation (3) employs dead reckoning to estimate the state of the robot; $\hat{R}_x$ is the position and direction of the robot estimated from the ith position, and u_{i-1} is the linear velocity of each wheel of the $i-1$th robot.

$\delta u_{i-1} \sim N$ can be expressed as the value of the normal distribution of disturbance applied to each wheel of the $i-1$th robot; the estimated state of the robot can be predicted by using the probability distribution.

Using equation (2), the state of the next robot can be expressed as equation (4), according to the current state, linear velocity, rotational speed, and sampling time

$$R_{i+1} = R_i + \begin{bmatrix} v_R \Delta t \cos\left(\varnothing_{R,i} + \frac{\omega_R \Delta t}{2}\right) \\ v_R \Delta t \sin\left(\varnothing_{R,i} + \frac{\omega_R \Delta t}{2}\right) \\ \omega_R \Delta t \end{bmatrix} \quad (4)$$

Utilizing equations (1) and (4), the dead reckoning navigation for predicting the state of the robot in the next step has the form of equation (5)

$$R_{i+1} = \begin{bmatrix} x_{R,i} \\ y_{R,i} \\ \theta_{R,i} \end{bmatrix} + \begin{bmatrix} \frac{\omega_r + \omega_l}{2} \cos\left(\theta_{R,i} + \frac{\omega_r - \omega_l}{2L}\right) \\ \frac{\omega_r + \omega_l}{2} \sin\left(\theta_{R,i} + \frac{\omega_r - \omega_l}{2L}\right) \\ \frac{\omega_r - \omega_l}{L} \end{bmatrix} \quad (5)$$

It is assumed without loss of generality that the rotational speed in the above equation is not affected by disturbance.

The motion of the mobile robot with torque is as follows

$$\bar{M}(R_i)\dot{v}_i + \bar{V}(R_i, \dot{R}_i)v_i + \bar{\tau}_{d,i} = \bar{B}\tau_i$$

where

$$\bar{M} = \left(\frac{r}{L}\right)^2 \begin{bmatrix} \left(m_i\left(\frac{L}{2}\right)_i^2 + I_i\right) + I_{w,i} & \left(m_i\left(\frac{L}{2}\right)_i^2 - I_i\right) \\ \left(m_i\left(\frac{L}{2}\right)_i^2 - I_i\right) & \left(m_i\left(\frac{L}{2}\right)_i^2 + I_i\right) + I_{w,i} \end{bmatrix}$$

$$m_i = m_{c,i} + 2m_{w,i}$$

$$I_i = m_{c,i} d_{c,i}^2 + 2m_{w,i}\left(\frac{L}{2}\right)^2 + I_{c,i} + 2I_{w,i}$$

$$\bar{V} = \begin{bmatrix} 0 & \frac{r^2}{L} m_{c,i} \dot{\theta}_{R,i} \\ -\frac{r^2}{L} m_{c,i} \dot{\theta}_{R,i} & 0 \end{bmatrix}, \bar{B} = \begin{bmatrix} 1 & 0 \\ 0 & 1 \end{bmatrix} \quad (6)$$

where mass regarding to robot body and wheel is $m_{c,i}$ and $m_{w,i}$, respectively. And inertia moments about robot body and wheel denoted by $I_{c,i}$, $I_{w,i}$, and $I_{w,i}$. $\bar{\tau}_{d,i}$ are unknown disturbances occurred by torque τ_i.

VRc and obstacle avoidance

VRc

Multi-robot navigation in formation has received extensive attention, with many works considering collision-free scenarios because multi-robot system shows obvious advantages over single robot, including greater flexibility, adaptability and robustness. Robots maintain specific formation while moving along path.

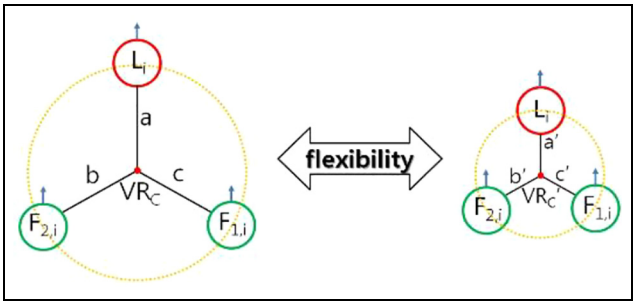

Figure 2. VRc of multi-robots.

In the proposed method, the center point VRc of a multi-robot formation is set using a constant distance "a" with reference to the leader robot; distances "b" and "c," which are the same distance as "a," are divided at the same angle around this point and are calculated according to the positions of follower robots 1 and 2. In this study, the distance "a" between VRc and the leader robot Li is the reference set distance, and "a" can be changed from its initial setting to accommodate the environment.

Figure 2 has a VRc resulting from the initial value "a" of the multi-robot formation. Here, "$a = b = c$," "a" is changed to "a'" if the size of the original formation is changed to accommodate the surrounding environment. As VRc is moved to the coordinates of VRc′, a change of formation is stably performed.

For flexible control of the multi-robot formation, the basic shape is formed by setting the initial value "a." For this purpose, a process is applied to the other scattered robots to be involved in the formation. After execution of decentralized control, the robots individually request information on other's states and then begin to move after deployment via centralized control. The conventional robot formation is formed at a predetermined position.[4] In this study, a formation is formed at not only a predetermined position but also during the robots' movement toward their targets. However, in this article, the formation is formed and maintained during the robots' movement as shown in Figure 3.

As shown in Figure 3, the motion of follower robots 1 and 2 is expressed by equations (7) and (8), respectively. The formation coordinates of the follower robots, calculated according to the initial value at any position, are set as the target states in the next step

$$\begin{bmatrix} x_{F_1,i} \\ y_{F_1,i} \\ \theta_{1,i} \end{bmatrix} = \begin{bmatrix} x_{F_1,i-1} - d_{f1}\cos(\theta_{1,i-1} + \alpha_1) \\ y_{F_1,i-1} - d_{f1}\sin(\theta_{1,i-1} + \alpha_1) \\ -(\theta_{1,i-1} + \alpha_1 - \theta_{1,i}) \end{bmatrix} \quad (7)$$

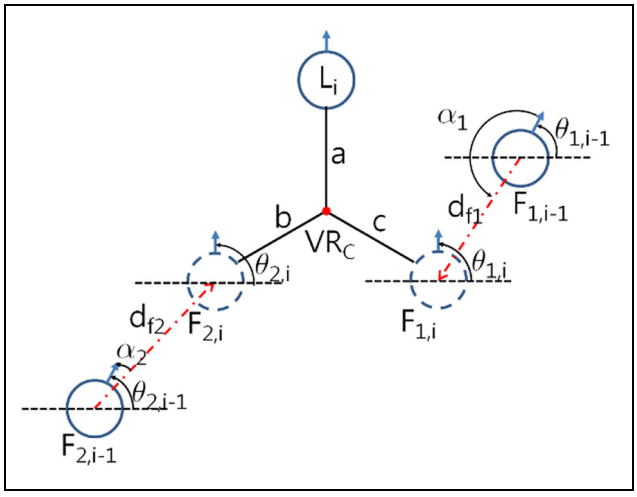

Figure 3. VRc formation control.

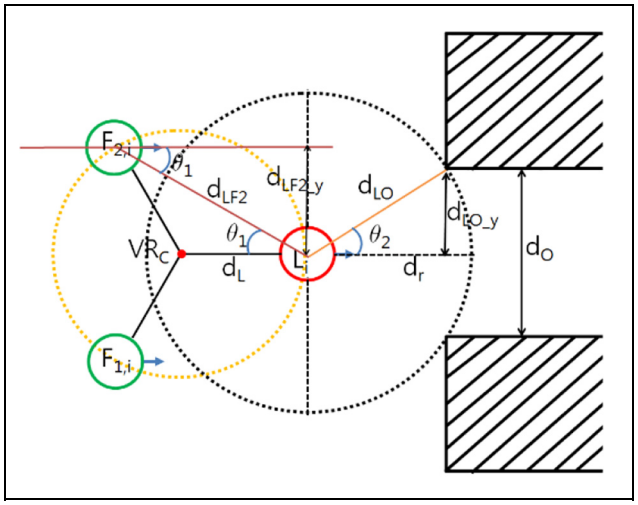

Figure 4. Obstacle avoidance of multi-robot formation.

$$\begin{bmatrix} x_{F_2,i} \\ y_{F_2,i} \\ \theta_{2,i} \end{bmatrix} = \begin{bmatrix} x_{F_2,i-1} - d_{f2}\cos(\theta_{2,i-1} - \alpha_2) \\ y_{F_2,i-1} - d_{f2}\sin(\theta_{2,i-1} - \alpha_2) \\ \dfrac{\pi}{2} - \theta_{2,i-1} \end{bmatrix} \tag{8}$$

When the robots set a formation, the position of a follower robot can be expressed by the coordinates of VRc and the distances b and c from the coordinates. The coordinates of the VRc can be represented by the current coordinates of the leader robot and the distance "a". The coordinates of the center point VRc are expressed as in equation (9) and the coordinates of follower robot 1 has the form of equation (10)

$$\begin{bmatrix} x_{VR_C,i} \\ y_{VR_C,i} \\ \varphi_{VR_C,i} \end{bmatrix} = \begin{bmatrix} x_{L,i} - a\cos(\varphi_{L,i}) \\ y_{L,i} - a\sin(\varphi_{L,i}) \\ \varphi_{L,i} \end{bmatrix} \tag{9}$$

$$x_{F_1,i} = x_{L,i} - a\cos\varphi_{L,i} - c\cos\rho_{F_1,i}$$

$$y_{F_1,i} = y_{L,i} - a\sin\varphi_{L,i} - c\sin\rho_{F_1,i}$$

$$\begin{bmatrix} x_{F_1,i} \\ y_{F_1,i} \\ \theta_{F_1,i} \end{bmatrix} = \begin{bmatrix} x_{L,i} - 2a\cos\left(\dfrac{\varphi_{L,i} + \rho_{F_1,i}}{2}\right)\cos\left(\dfrac{\varphi_{L,i} - \rho_{F_1,i}}{2}\right) \\ y_{L,i} - 2a\sin\left(\dfrac{\varphi_{L,i} + \rho_{F_1,i}}{2}\right)\cos\left(\dfrac{\varphi_{L,i} - \rho_{F_1,i}}{2}\right) \\ \theta_{L,i} \end{bmatrix} \tag{10}$$

In equation (10), $\varphi_{L,i}$ is the ith heading of the leader robot and $\rho_{F_1,i}$ is the ith angle between the VRc and follower robot 1. Because $a = b = c$ as shown in Figures 2 and 3, it can be described as equation (10). Based on the above descriptions, the coordinates of follower robot 2 has the form of equation (11)

$$\begin{bmatrix} x_{F_2,i} \\ y_{F_2,i} \\ \theta_{F_2,i} \end{bmatrix} = \begin{bmatrix} x_{L,i} + 2a\cos\left(\dfrac{\varphi_{L,i} + \rho_{F_2,i}}{2}\right)\cos\left(\dfrac{\varphi_{L,i} - \rho_{F_2,i}}{2}\right) \\ y_{L,i} - 2a\sin\left(\dfrac{\varphi_{L,i} + \rho_{F_2,i}}{2}\right)\cos\left(\dfrac{\varphi_{L,i} - \rho_{F_2,i}}{2}\right) \\ \theta_{L,i} \end{bmatrix} \tag{11}$$

Obstacle and collision avoidance

Obstacle avoidance. Robots in a formation must perform complex maneuvers to avoid or pass obstacles while maintaining the formation. When the robots in formation move, the leader robot leads the follower robots, detects and judges obstacles, and avoids and passes through obstacles while deforming the formation fluidly.

As shown in Figure 4, in order to pass through the space between two obstacles, the robot group formed should consider the following parameters: distance d_{LF_2} and direction angle θ_1 between the leader and follower robots, the detection distance d_r of the leader robot, distance d_{LO} and direction angle θ_2 between the leader robot and the obstacle, and space height d_O between two obstacles. The conditions for passing two obstacles are described as follows.

1. Condition of minimum formation: $d_{L,i} \geqslant L/2$
2. $d_{L,i} < d_{r,i}, d_{LF_y,i} < d_{LO_y,i}$
3. $d_{LF_2,i} < d_{LO,i}, \theta_{1,i} < \theta_{2,i}$
4. $(d_{LF_2,i} + L/2) < d_{LO_y,i}$ or $(d_{F_2F_1,i} + L) \leqslant d_O$
5. if, $d_{r,i} \geqslant d_{LO,i}$ and $(L/2) \leqslant d_{L,i} < d_{LO_y,i}$
   $d_{L,i} = d_{LO,i}$
   if, $d_{O,i} = d_{F_2F_1,i} + L$
   $d_{L,i} = d_{O,i} - L$

The position and angle of each robot and obstacle are calculated using equations (12) and (13), which respectively, take the form of the Pythagorean Theorem and the cosine second law

$$d_{LF_2} = \sqrt{(x_{L,i} - x_{F_2,i})^2 + (y_{L,i} - y_{F_2,i})^2} \tag{12}$$

$$\theta_1 = \cos^{-1}\left(\frac{d_L^2 + d_{LF_2}^2 - d_{F_2VR_C}^2}{2d_L d_{LF_2}}\right) \tag{13}$$

Collision avoidance. When robots in formation change their directions to reform the formation, if the trajectories of two follower robots overlap, there is a risk of collision. In this case, we use the repulsive force of a potential field[15,16] to set a new waypoint for avoiding collisions and then use an attractive force to retrieve the path.

The attractive potential energy (U_a) and attractive force (F_a) for the follower robot can be expressed by equation (14) for $i = 1, 2, 3, \ldots, n$, where i is the robot number

$$\begin{aligned}
&f_i = \begin{bmatrix} x_{fi} & y_{fi} \end{bmatrix}^T,\ f_{t_i} = \begin{bmatrix} x_{f_{t_i}} & y_{f_{t_i}} \end{bmatrix}^T \\
&U(f_i) = U_a(f_i) + \sum U_r(f_i) \\
&\text{if } f_i > f_{t_i} \\
&\quad U_a(f_i) = \frac{1}{2} K_a (f_i - f_{t_i})^2 \\
&\quad F_{a_i} = -K_a (f_i - f_{t_i}) \\
&\text{Else if } f_i \leqslant f_{t_i} \\
&\quad U_a(f_i) = 0 \\
&\quad F_{a_i} = 0 \\
&\text{End}
\end{aligned} \tag{14}$$

Equation (15) represents the repulsive potential energy (U_r) and repulsive force (F_r) of the follower robot

$$\begin{aligned}
&\text{if } \|f_i - f_{i\pm1}\| \leqslant d_0 \\
&\quad U_r(f_i) = \frac{1}{2} K_r \left(\frac{1}{\|f_i - f_{i\pm1}\|} - \frac{1}{d_0} \right)^2 \\
&\quad F_{r_i} = K_r \left(\frac{1}{\|f_i - f_{i\pm1}\|} - \frac{1}{d_0} \right) \times \frac{1}{\|f_i - f_{i\pm1}\|^2} \times \frac{\partial \|f_i - f_{i\pm1}\|}{\partial f_i} \\
&\text{Else if } \|f_i - f_{i\pm1}\| > d_0 \\
&\quad U_r(f_i) = 0 \\
&\quad F_{r_i} = 0 \\
&\text{End}
\end{aligned} \tag{15}$$

f_i and f_{t_i} are the follower robot and the target point of the follower robot, respectively. K_a and K_r are the respective potential constants. ($\|f_i - f_{t_i}\|$) is the distance from the current state to the target. $\|f_i - f_{t_i}\|$ is the shortest distance to other robots or obstacles in the current state, and d_0 is the distance constant indicating the degree of separation from the object to be avoided.

Equations (14) and (15) are applied not only for collision avoidance between robots but also for obstacle avoidance. Using these equations, a new safe waypoint can be calculated.

Movement technique

Adaptive controllers

Define the waypoint model of the robot as

$$\dot{x}_{w,i} = v_{w,i} \cos \theta_{w,i} \tag{16}$$

$$\dot{y}_{w,i} = v_{w,i} \sin \theta_{w,i} \tag{17}$$

$$\dot{\theta}_{w,i} = \omega_{w,i} \tag{18}$$

where $v_{w,i}$ and $\omega_{w,i}$ are the desired linear and angular velocities, respectively. The tracking error is defined as $E_{q,i} = [x_{w,i} - x_{c,i}, y_{w,i} - y_{c,i}, \theta_{w,i} - \theta_{c,i}]^T$. The derivative of the tracking error can be described as

$$\begin{aligned}
\dot{E}_{q,i} = \begin{bmatrix} \dot{x}_{E,i} \\ \dot{y}_{E,i} \\ \dot{\theta}_{E,i} \end{bmatrix} &= \begin{bmatrix} -1 \\ 0 \\ 0 \end{bmatrix} v_{C,i} + \begin{bmatrix} y_{E,i} \\ -x_{E,i} \\ -1 \end{bmatrix} \omega_{C,i} \\
&+ \begin{bmatrix} v_{w,i} \cos \theta_{E,i} \\ v_{w,i} \sin \theta_{E,i} \\ \omega_{w,i} \end{bmatrix}
\end{aligned} \tag{19}$$

As shown in Kanayama et al.,[17] the linear and angular velocities are transferred as the following equation

$$\begin{bmatrix} v_{f,i} \\ \omega_{f,i} \end{bmatrix} = \begin{bmatrix} v_{w,i} \cos \theta_{E,i} + K_{1,i} x_{E,i} \\ \omega_{w,i} + K_{2,i} v_{w,i} y_{E,i} + K_{3,i} \sin \theta_{E,i} \end{bmatrix} \tag{20}$$

where $K_{1,i}$, $K_{2,i}$, and $K_{3,i}$ are the positive constants. Using equation (1), equation (19) can be reformed as

$$\begin{aligned}
\dot{E}_{q,i} = &\begin{bmatrix} -\frac{r_i}{2} + \frac{r_i}{L_i} y_{E,i} \\ -\frac{r_i}{L_i} x_{E,i} \\ -\frac{r_i}{L_i} \end{bmatrix} v_{1,i} + \begin{bmatrix} -\frac{r_i}{2} + \frac{r_i}{L_i} y_{E,i} \\ \frac{r_i}{L_i} x_{E,i} \\ \frac{r_i}{L_i} \end{bmatrix} v_{2,i} \\
&+ \begin{bmatrix} v_{w,i} \cos \theta_{E,i} \\ v_{w,i} \sin \theta_{E,i} \\ \omega_{w,i} \end{bmatrix}
\end{aligned} \tag{21}$$

To obtain the angular velocities of each wheels, parameters r and L are needed

$$\begin{aligned}
v_{c,i} &= \begin{bmatrix} \hat{a}_{1,i} & \hat{a}_{2,i} \\ \hat{a}_{1,i} & -\hat{a}_{2,i} \end{bmatrix} \begin{bmatrix} v_{f,i} \\ \omega_{f,i} \end{bmatrix} \\
&= \begin{bmatrix} a_{1,i} + \tilde{a}_{1,i} & a_{2,i} + \tilde{a}_{2,i} \\ a_{1,i} + \tilde{a}_{1,i} & -a_{2,i} - \tilde{a}_{2,i} \end{bmatrix} \begin{bmatrix} v_{f,i} \\ \omega_{f,i} \end{bmatrix}
\end{aligned} \tag{22}$$

where $\hat{a}_{1,i}$ and $\hat{a}_{2,i}$ are the estimate of $a_{1,i}$ and $a_{2,i}$. Equation (21) can be described as

$$\dot{E}_{q,i} = \left(1 + \frac{\tilde{a}_{1,i}}{a_{1,i}}\right)\begin{bmatrix} -v_{f,i} \\ 0 \\ 0 \end{bmatrix} + \left(1 + \frac{\tilde{a}_{2,i}}{a_{2,i}}\right)\omega_{f,i} \begin{bmatrix} y_{E,i} \\ -x_{E,i} \\ -1 \end{bmatrix} + \begin{bmatrix} v_{w,i}\cos\theta_{E,i} \\ v_{w,i}\sin\theta_{E,i} \\ \omega_{w,i} \end{bmatrix} \tag{23}$$

To design $\hat{a}_{1,i}$ and $\hat{a}_{2,i}$, the Lyapunov function is defined as

$$V_1 = \frac{1}{2}\left(x_{E,i}^2 + y_{E,i}^2\right) + \frac{(1-\cos\theta_{E,i})}{K_{2,i}} + \frac{\tilde{a}_{1,i}^2}{2\gamma_{1,i}a_{1,i}} + \frac{\tilde{a}_{2,i}^2}{2\gamma_{2,i}a_{2,i}} \tag{24}$$

For Lyapunov stability of the system, the parameters are designed as

$$\dot{\hat{a}}_{1,i} = \gamma_{1,i}x_{E,i}v_{f,i}, \quad \dot{\hat{a}}_{2,i} = \gamma_{2,i}\frac{\omega_{f,i}\sin\theta_{E,i}}{K_{2,i}} \tag{25}$$

The differentiation of V_1 is non-negative as shown in equation (26)

$$\begin{aligned} \dot{V}_1 &= x_{E,i}\dot{x}_{E,i} + y_{E,i}\dot{y}_{E,i} + \frac{\dot{\theta}_{E,i}\sin\theta_{E,i}}{K_{2,i}} + \frac{\tilde{a}_{1,i}\dot{\tilde{a}}_{1,i}}{\gamma_{1,i}a_{1,i}} + \frac{\tilde{a}_{2,i}\dot{\tilde{a}}_{2,i}}{\gamma_{2,i}a_{2,i}} \\ &= -K_{1,i}x_{E,i}^2 - \frac{K_{3,i}(\sin\theta_{E,i})^2}{K_{2,i}} + \frac{\tilde{a}_{1,i}}{\gamma_{1,i}a_{1,i}}\left(\dot{\hat{a}}_{2,i} - \gamma_{2,i}\frac{\omega_{f,i}\sin\theta_{E,i}}{K_{2,i}}\right) \\ &= -K_{1,i}x_{E,i}^2 - \frac{K_{3,i}(\sin\theta_{E,i})^2}{K_{2,i}} \leqslant 0 \end{aligned} \tag{26}$$

As $t \to \infty$, $E_{q,i}$ is shown to be a stable equilibrium point.

The velocity tracking errors $E_{c,i}$ of the robot are

$$E_{c,i} = v_i - v_{c,i} = \begin{bmatrix} v_{1,i} - v_{1c,i} \\ v_{2,i} - v_{2c,i} \end{bmatrix} \tag{27}$$

Equation (6) is rewritten as

$$\bar{M}\left(\dot{v}_{c,i} + \dot{E}_{c,i}\right) + \bar{V}(v_{c,i} + E_{c,i}) + \bar{\tau}_{d,i} = \bar{B}\tau_i \tag{28}$$

Then

$$\begin{aligned} \bar{M}\dot{E}_{c,i} &= -(\bar{M}\dot{v}_{c,i} + \bar{V}v_{c,i}) - \bar{V}E_{c,i} - \bar{\tau}_{d,i} + \bar{B}\tau_i \\ &= -Y_{c,i}P_i - \bar{V}E_{c,i} - \bar{\tau}_{d,i} + \bar{B}\tau_i \end{aligned} \tag{29}$$

The torque controller is defined as

$$\tau_i = \bar{B}^{-1}\left(-K_{d,i}E_{c,i} + Y_{c,i}\hat{P}_i - u_{s,i}\right) \tag{30}$$

where

$$\bar{M}\dot{v}_{c,i} + \bar{V}v_{c,i} = Y_{c,i}P_iY_{c,i} = \begin{bmatrix} \dot{v}_{1c,i} & \dot{v}_{2c,i} & \dot{\theta}_i v_{2c,i} \\ \dot{v}_{2c,i} & \dot{v}_{1c,i} & -\dot{\theta}_i v_{1c,i} \end{bmatrix}$$
$$P_i = \begin{bmatrix} \frac{r_i^2}{L_i^2}\left(m_i\frac{L_i}{2}^2 + I_i\right) + I_{w,i} & \frac{r_i^2}{L_i^2}\left(m_i\frac{L_i}{2}^2 - I_i\right) & \frac{r_i^2}{L_i}m_{c,i} \end{bmatrix}^T \tag{31}$$

To obtain the torque controller, the Lyapunov function is defined as

$$V_2 = V_1 + \frac{1}{2}E_{c,i}^T\bar{M}E_{c,i} + \frac{1}{2}\tilde{P}_i^T\Gamma^{-1}\tilde{P}_i + \frac{\tilde{c}_{0,i}^2}{2\gamma_{3,i}} + \frac{\tilde{c}_{1,i}^2}{2\gamma_{4,i}} \tag{32}$$

The parameters are selected as

$$\dot{\hat{P}}_2 = -\Gamma Y_{c,i}^T E_{c,i},\ \dot{\hat{c}}_{0,i} = \gamma_{3,i}\|E_{c,i}\|,\ \dot{\hat{c}}_{1,i} = \gamma_{4,i}\|v_i\|\|E_{c,i}\| \tag{33}$$

The differential of V_2 is

$$\begin{aligned} \dot{V}_2 &= \dot{V}_1 - E_{c,i}^T K_{d,i}E_{c,i} - E_{c,i}^T\bar{\tau}_{d,i} - AE_{c,i}^T\mathrm{sgn}(E_{c,i}) + \frac{\tilde{c}_{0,i}\dot{\tilde{c}}_{0,i}}{\alpha_{0,i}} + \frac{\tilde{c}_{1,i}\dot{\tilde{c}}_{1,i}}{\alpha_{1,i}} \leqslant \dot{V}_1 \\ &- E_{c,i}^T K_{d,i}E_{c,i} - (A - \|\bar{\tau}_{d,i}\|)\|E_{c,i}\| + \frac{\tilde{c}_{0,i}\dot{\tilde{c}}_{0,i}}{\alpha_{0,i}} + \frac{\tilde{c}_{1,i}\dot{\tilde{c}}_{1,i}}{\alpha_{1,i}} \leqslant \dot{V}_1 - E_{c,i}^T K_{d,i}E_{c,i} \\ &- \tilde{c}_{0,i}\left(\|E_{c,i}\| - \frac{\dot{\tilde{c}}_{0,i}}{\alpha_{0,i}}\right) - \tilde{c}_{1,i}\left(\|v_i\|\|E_{c,i}\| - \frac{\dot{\tilde{c}}_{1,i}}{\alpha_{1,i}}\right) \\ &= \dot{V}_1 - E_{c,i}^T K_{d,i}E_{c,i} \leqslant 0 \end{aligned} \tag{34}$$

$E_{q,i} = 0$ is an asymptotically stable point as $t \to \infty$.

Formation switching method

The formation switching method is determined by heading change of the leader robot. In Figure 5(a), if the leader robot rapidly changes its heading to follow the path, the $i + n$th waypoint of the follower robot suddenly changes. As a result, follower robots will excessively move to track their waypoints, but they may fail to follow their paths, depending on the robot's platform. In this case, the robots should use the proposed formation switching method to track their trajectories, as shown in Figure 5(b). Conclusively, if the heading angle of the leader robot is $-(\pi/2) < R_\theta < (\pi/2)$, the existing formation is maintained. However, if heading angle of the leader robot, R_θ, satisfies the condition of

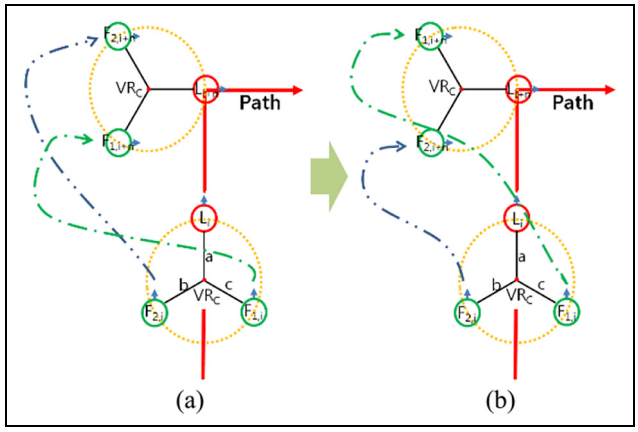

Figure 5. (a) Basic formation and (b) formation switching movement.

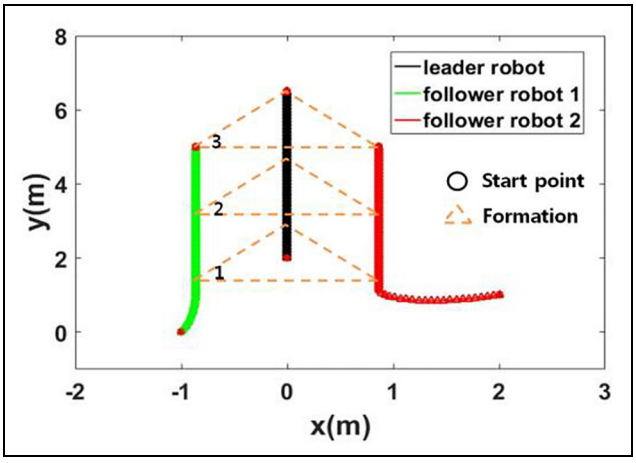

Figure 7. Formation configuration while moving.

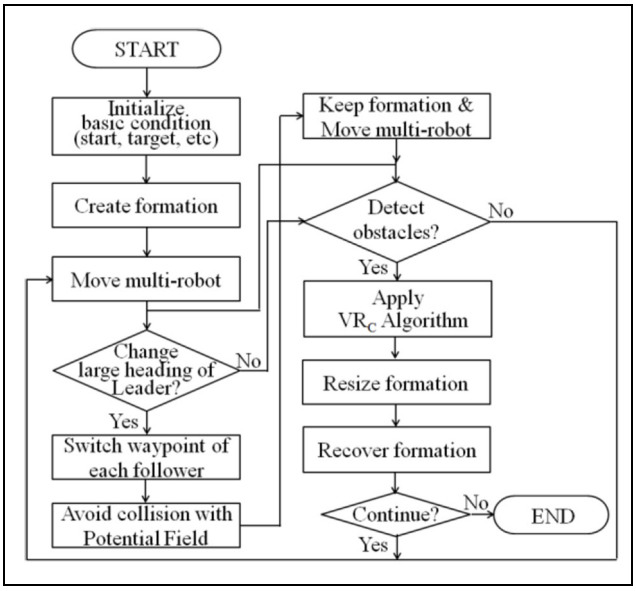

Figure 6. System block diagram.

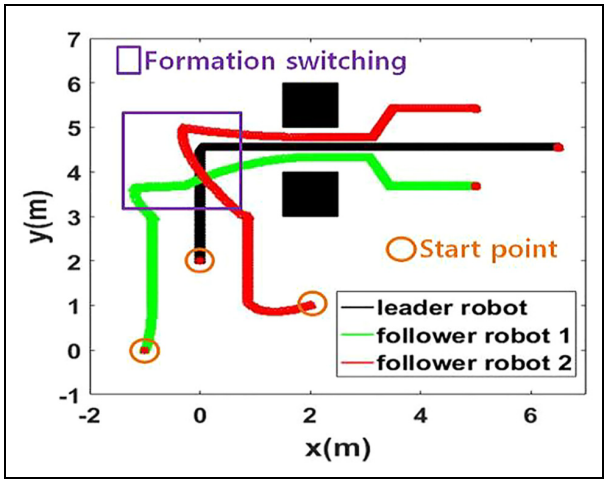

Figure 8. Formation switching and VRc of multi-robot formation.

$(\pi/2)\sim 2\pi \leqslant R_\theta \leqslant -(\pi/2)\sim 2\pi$, follower robots follow a changed waypoint position using small posture changes and move while keeping the original formation.

System block diagram

System block diagram of the entire multi-robot system proposed in this article is shown in Figure 6.

Simulation

In this simulation, robots use the proposed VRc method to form and maintain a formation. For this purpose, follower robots switch their tracking paths according to the heading angle of the leader robot. When an obstacle is detected, the formation size is reduced step-by-step in order to pass through the obstacle area. After passing through the obstacles, the robots reform their original formation and continue their mission.

Figure 7 shows the process of multi-robot formation while moving. First, the starting points of the leader robot and follower robots 1 and 2 are, respectively, defined as $L = (0\ 2\ \pi/2)^T$, $F_1 = (-1\ 0\ \pi/2)^T$, and $F_2 = (2\ 1\ \pi/2)^T$. While the leader robot moves in a straight path, the follower robots form an initial formation in one region according to the formation command and maintain the formation continuously.

Second, when the leader suddenly changes its angle from $\pi/2$ to 0° at 4.5 m, the follower robots simultaneously change their waypoints and form a formation with the leader robot, using the above-mentioned switching method. Comparing with Dai et al.,11 when the leader robot turns sharp angle, the follower robots can follow leader robot to effectively reform the formation with leader robot as shown in Figure 8, where the three robots form a stable and smooth formation.

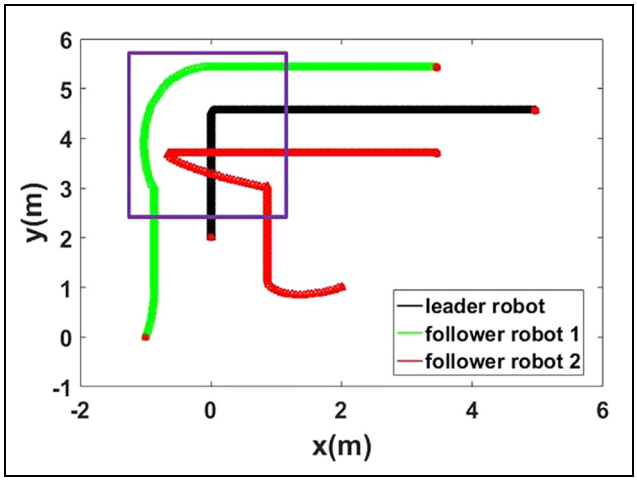

Figure 9. Excessive movement of follower robots in case of sudden posture change of leader robot.

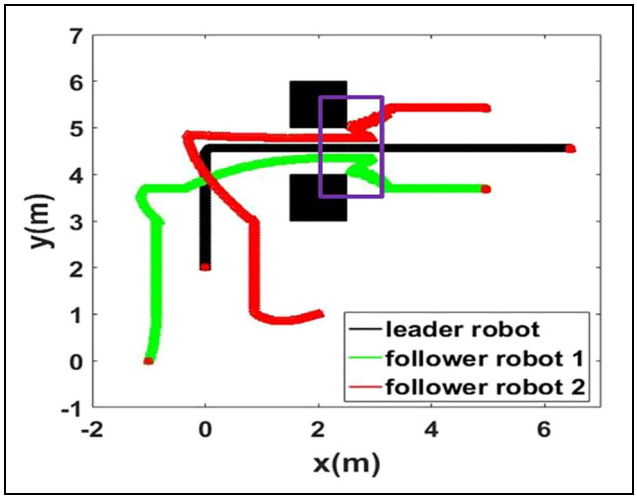

Figure 10. Collision errors occurred when restoring a multi-robot formation.

As shown in Figure 9 where the switching method is not applied, the follower robots cannot follow the leader robot properly due to excessive postural changes. Moreover, it is difficult to maintain the formation size.

Third, the formation size can be adjusted by moving the VRc of the robots. As shown in Figure 8, when the leader robot detects the obstacle, it judges whether it can pass through the obstacle by using the proposed method. By determining the distance between two obstacles, the robots can shrink the formation to pass through the obstacles. It can be confirmed that the deformation starts at the 0 point on the x-axis, and the formation scale is reduced at the 2–4 points. After passing through the obstacles, the formation restoration is performed. If the formation size is enlarged suddenly, ineffective movements of follower robots may occur as shown in Figure 10. To prevent this problem, as shown in Figure 8, the size of the formation is gradually increased with consideration of the formation size and the robots' speeds.

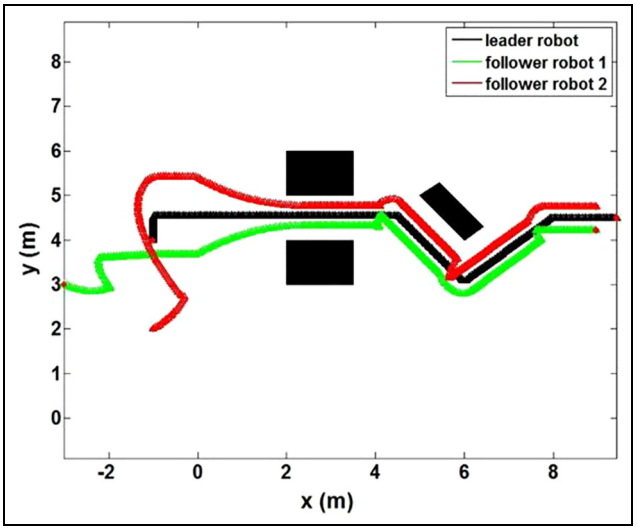

Figure 11. Avoidance path for robots when obstacles are detected.

Finally, as shown in Figure 11, if the robot confronts another obstacle after passing through the obstacles, the robots avoid collision with the obstacle and continue generating their paths. The starting points of each robot are $L = (-1 \quad 4 \quad \pi/2)^T$, $F_1 = (-3 \quad -3 \quad \pi/2)^T$, and $F_2 = (-1 \quad 2 \quad \pi/2)^T$, respectively. The obstacles are depicted as follows $O_1 = \begin{bmatrix} 2 & 2 & 3.5 & 3.5 \\ 4 & 3 & 3 & 4 \end{bmatrix}$, $O_2 = \begin{bmatrix} 2 & 2 & 3.5 & 3.5 \\ 5 & 6 & 6 & 5 \end{bmatrix}$, and $O_3 = \begin{bmatrix} 5 & 6 & 6.433 & 5.433 \\ 5 & 4 & 4.3 & 5.3 \end{bmatrix}$. The robots' safe range and the detection radius are set to be $1.5 \times \sin(\pi/4)$ and $1.5 \times \sin(\pi/4) + 0.005$, respectively. The distance between the leader robot and VRc in the initial formation is set to be 1 m. When new obstacle is detected after passing through the obstacles, the robots' formation size cannot be maintained because the follower robot's posture changes. However, as shown in Figure 11, after detecting obstacles based on the robots' VRc, follower robots can prevent collisions with obstacles and the robots' formation size can be adjusted using the VRc.

Figure 12 shows the tracking error of each robot when it follows the path. Figure 12(a) depicts the state error of the leader robot after 0.5 m was added to the x value of the current leader robot coordinates. As shown in the result, when the third obstacle is avoided, the leader robot is maintaining a distance of about 0.5 m, except for the new created path. The y value and the heading angle are finally maintained at 0, and it is clear that there is no error. Figure 12(b) and (c) shows the

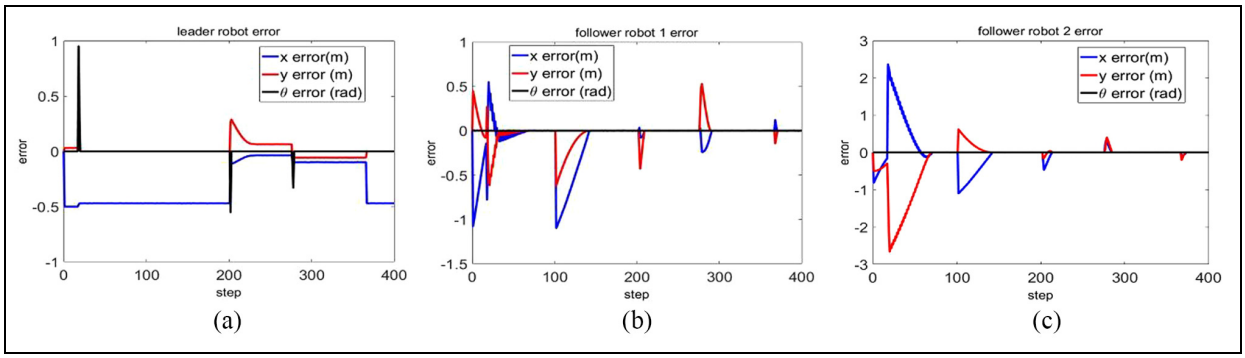

Figure 12. Tracking errors: (a) leader robot, (b) follower robot 1, and (c) follower robot 2.

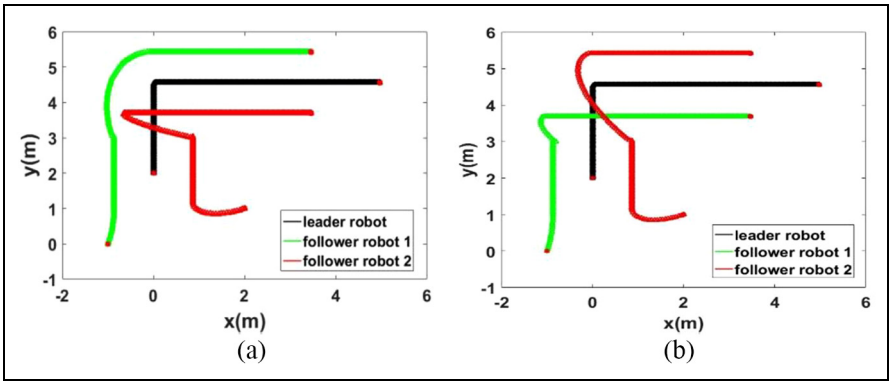

Figure 13. Comparison of results for (a) switching and (b) non-switching formation.

state errors of follower robots 1 and 2 that result from following a path created by the leader robot. In conclusion, follower robots 1 and 2 effectively track the generated paths because their state errors converge to zero.

Figure 13 shows comparison results of non-switching and switching formation under the same condition. The elapsed time of navigation in formation results for non-switching and switching formation is 29.927 and 29.888 s, respectively. In case of non-switching formation, when robots' position is switched, follower robots' heading is changed rapidly, and then, actually robots' formation cannot restore quickly enough as shown in Figure 13(a). However, the proposed method as shown in Figure 13(b), switching formation, can solve the problem in Figure 13(a).

Experiment

In this chapter, we validate the proposed algorithm through experiments and evaluate the result through data analysis. The experimental conditions are as follows.

- Map size: 6 m × 8 m
- Hardware: Kobuki robots
- Software: LabVIEW, MathScript
- Shared network: Wifi
- Obstacle size: 1 m × 1 m × 0.5 m

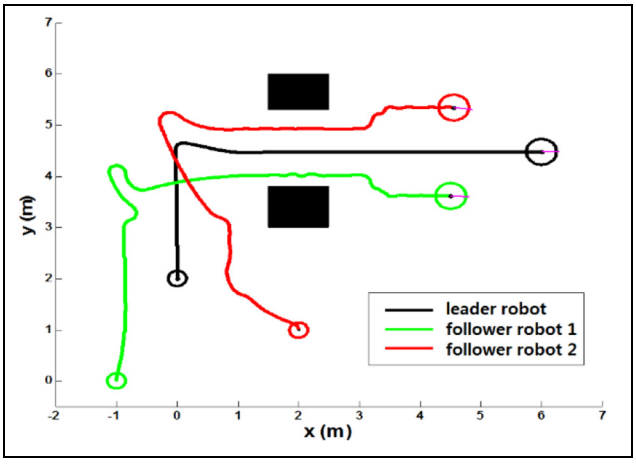

Figure 14. Experiment result: the three robots' trajectories to avoid two obstacles.

The Kobuki base has the following specification: a maximum linear velocity of 0.7 m/s, a maximum

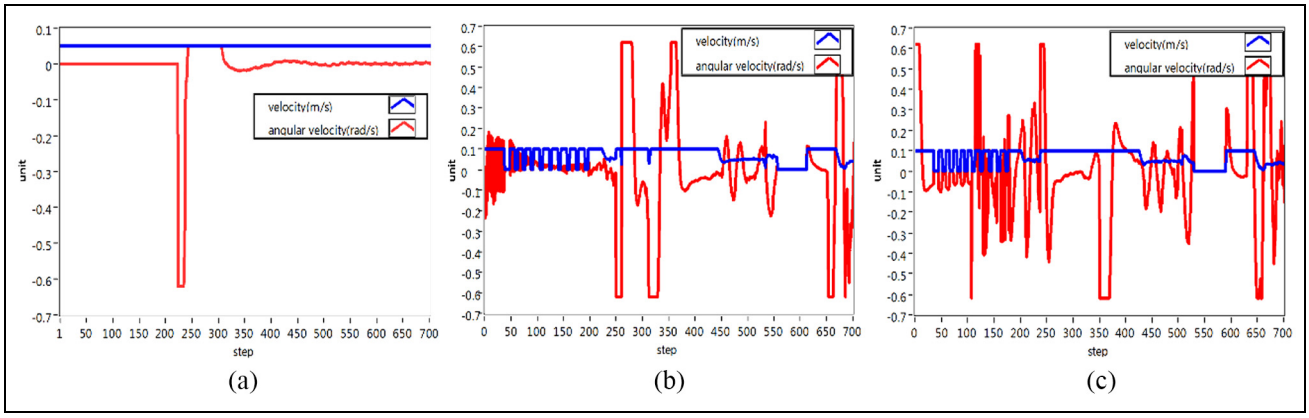

Figure 15. Linear and angular velocities of leader and follower robots: (a) leader robot, (b) follower robot 1, and (c) follower robot 2.

rotation speed of 180°/s, a payload of 5 kg, a wheel radius of 95 mm, and a distance between wheels of 263 mm.

Figure 14 which depicts experiment result in the same environment as of Figure 8 shows three robots' trajectories as they avoid two obstacles. When the leader robot tracks a predetermined path, two follower robots navigate in formation to follow the leader robot using the variable VRc. When the leader robot changes its heading direction for more than a certain angle, the two follower robots rapidly switch their tracking positions to reform the formation. In addition, when the leader robot detects an obstacle, the formation size is gradually reduced by the VRc and restored for the robots to pass the obstacles successfully.

The starting points of the leader robot and follower robots 1 and 2 are defined as $L = (0 \quad 2 \quad \pi/2)^T$, $F_1 = (-1 \; 0 \; \pi/2)^T$, and $F_2 = (2 \; 1 \; \pi/2)^T$, respectively. The leader robot's maximum linear and angular velocities are 0.05 m/s and 0.62 rad/s, respectively. Those of the follower robots are 0.1 m/s and 0.62 rad/s.

Figure 15 shows the linear and angular velocity of the leader robot following the path and the linear and angular velocities of the two follower robots as they follow the generated waypoints according to the leader's movement. The leader robot moves forward at a constant linear velocity and changes its angular velocity to rotate 90°. The follower robots, located at different starting points, quickly follow the leader robot by changing their linear velocity v and angular velocity ω. As shown in Figure 16, the distances between the leader robot and the follower robots present the formation maintenance and tracking process of the robots. The default distance from the leader robot to the VRc is 1 m; the formation's basic shape is triangular, and the distance and angle between the leader and each follower robot is 1.7 m and 60°. When an obstacle is detected, VRc is decreased by measuring the distance

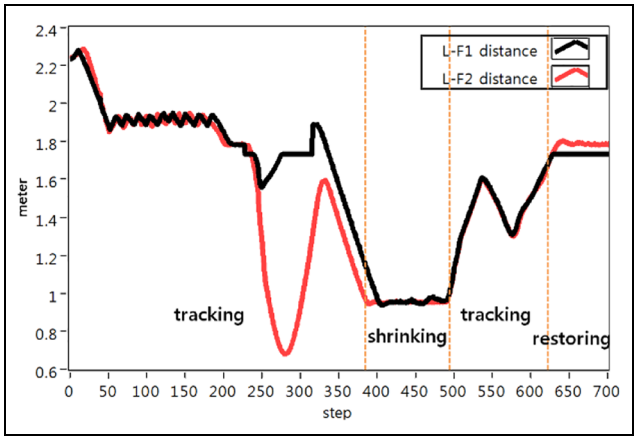

Figure 16. Distance between leader robot and follower robots.

from the obstacle. At this time, the distance from the VRc to the leader is 0.55 m, and the distance and angle between the leader and follower robots is 0.95 m and 60°. Initially, the three robots successfully form and maintain the initial formation. When the leader robot detects the obstacles, the three robots respond by shrinking the formation. After passing through the obstacles, the three robots restore the original formation. Figure 17 shows snapshots of the experimental results based on the proposed algorithm and the data in Figures 14–16.

Conclusion

In this study, we suggested a variable formation control of multiple robots via VRc and formation switching to accommodate large heading changes by leader robot and verified the effectiveness of the proposed algorithm for multi-robot collaboration by grouping. The

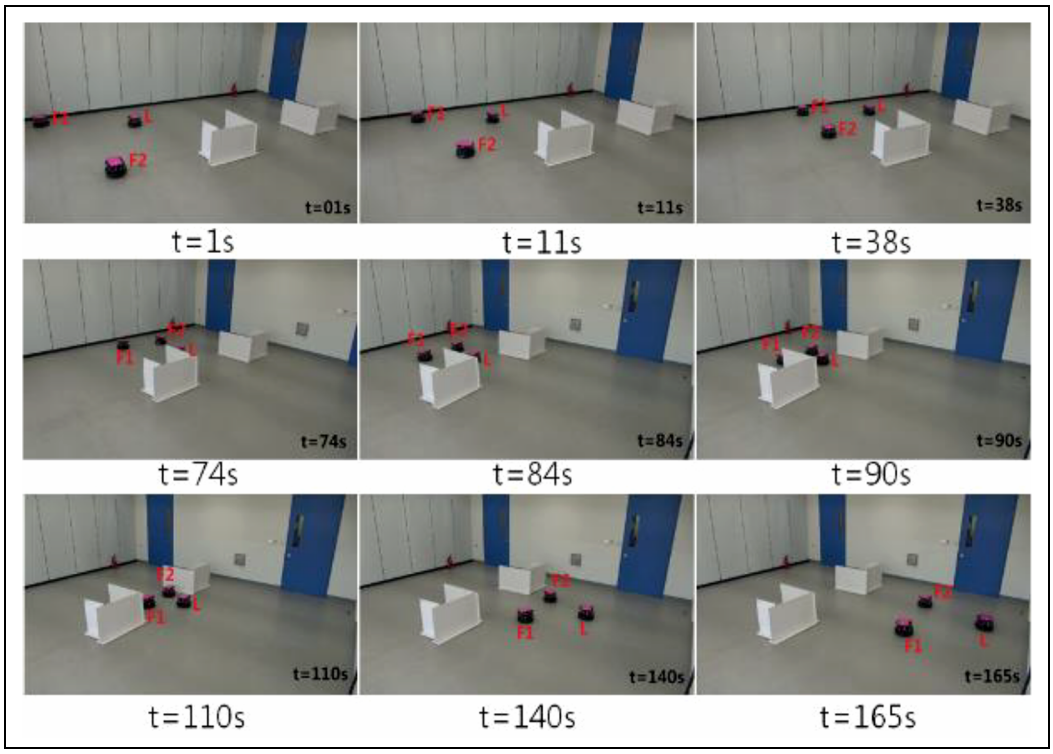

Figure 17. Flexible formation and position switching of robots in real environment.

proposed method consists of three main tasks: formation switching, VRc control, and formation restoration. Through effective formation control, multiple robots act like a single robot. These robots are able to (1) avoid collisions with each other, (2) create and change formations, and (3) decide the best safe plan by determining the shape of an obstacle. Multi-robot formation under communication constraints between robots and complex three-dimensional (3D) environment is undergoing. In future studies, we will conduct intelligent control research and apply the control algorithm not only in group level but also in individual level under moving obstacle environment.

Declaration of conflicting interests

The author(s) declared no potential conflicts of interest with respect to the research, authorship, and/or publication of this article.

Funding

The author(s) disclosed receipt of the following financial support for the research, authorship, and/or publication of this article: This work was supported by the 2015 Yeungnam University Research Grant.

ORCID iD

Yanyan Dai https://orcid.org/0000-0003-2484-4585

References

1. Liang X, Liu Y, Wang H, et al. Leader-following formation tracking control of mobile robots without direct position measurements. *IEEE Trans Automat Contr* 2016; 61: 4131–4137.
2. Lee S and Myung H. Receding horizon particle warm optimisation-based formation control with collision avoidance for non-holonomic mobile robots. *IET Contr Theror Appli* 2015; 9: 2075–2083.
3. Tian J, Luo H, Sun W, et al. Sliding mode control with gain-scheduled and improved boundary layer for nonholonomic multi-robot formation. In: *Proceedings of the 35th Chinese control conference*, Chengdu, China, 27–29 July 2016, pp.608–613. New York: IEEE.
4. Jin J, Kim Y, Wee S, et al. Consensus based attractive vector approach for formation control of nonholonomic mobile robots. In: *IEEE international conference on AIM*, Busan, South Korea, 7–11 July 2015, pp.997–983. New York: IEEE.
5. Xia S, Feng V, Lian H, et al. Dynamic formation and obstacle avoidance control for multi robot system. In: *World congress on intelligent control and automation (WCICA)*, Guilin, China, 12–15 June 2016, pp.59–63. New York: IEEE.
6. Alonso-Mora J, Montijano E, Schwager M, et al. Distributed multi-robot formation control among obstacles: a geometric and optimization approach with consensus. In: *IEEE international conference on robotics and automation (ICRA)*, Stockholm, 16–21 May 2016, pp 5356–5363. New York: IEEE.

7. Jia Y, Xianonanr W and Xin Y. Adaptive conversion of the leader in multi-robot obstacle avoidance. In: *Proceedings of the 26th Chinese control and decision conference (2014 CCDC)*, Changsha, China, 31 May–2 June 201, pp.375–377. New York: IEEE.
8. Baranzadeh A and Nazarzehi V. A decentralized formation building algorithm with obstacle avoidance for multi-robot systems. In: *IEEE international conference on robotics and biomimetics (ROBIO)*, Zhuhai, China, 6–9 December 2105, pp.2513–2518. New York: IEEE.
9. Jin J, Green A and Gans N. A stable switched-system approach to obstacle avoidance for mobile robots in SE(2). In: *International conference on intelligent robots and systems*, Chicago, IL, 14–18 September 2014, pp.1533–1539. New York: IEEE.
10. Jin J, Gans N, Kim Y, et al. A switched-system approach to shared robust control and obstacle avoidance for mobile robots. In: *ASME 2014 dynamic systems and control conference*, San Antonio, TX, 22–24 October 2014, pp.1–10. New York: IEEE.
11. Dai Y, Lee S, Kim Y, et al. A switching formation strategy for obstacle avoidance of multi-robot system. In: *Proceedings of the 4th annual IEEE international conference on cyber technology in automation, control and intelligent*, Hong Kong, China, 4–7 June 2014, pp.457–462. New York: IEEE.
12. Dai Y, Kim Y, Wee S, et al. A switching formation strategy for obstacle avoidance of a multi-robot system based on robot priority model. *ISA Trans* 2015; 56: 123–134.
13. Das T and Kar IN. Design and implementation of an adaptive fuzzy logic-based controller for wheeled mobile robots. *IEEE Trans Control Syst Tech* 2016; 14: 501–510.
14. Campion G, Bastin G and D'Andrea-Novel B. Structural properties and classification of kinematic and dynamic models of wheeled mobile robots. In: *Proceedings IEEE international conference on robotics and automation*, Atlanta, GA, 2–6 May 1996, pp.47–62. New York: IEEE.
15. Osorio-Comparan R, Lopez-Juarez I, Reyes-Acosta A, et al. Mobile Robot Navigation using Potential Field and LMA. In: *International conference on automatic*, Curico, Chile, 19–21 October, pp.1–7. New York: IEEE.
16. Shi P and Zhao Y. Global Path Planning for Mobile Robot Based on Improved Artificial Potential Function. In: *International conference on automation and logistics*, Shenyang, China, 5–7 August 2009, pp.1900–1904. New York: IEEE.
17. Kanayama Y, Kimura Y, Miyazaki F, et al. A stable tracking control method for a nonholonomic mobile robot. In: *Proceedings IROS '91: IEEE/RSJ international workshop on intelligent robots and systems '91*, Osaka, Japan, 3–5 November 1991, pp.1236–1241. New York: IEEE.